

Synthesis of Hierarchically Copper Cobalt Sulfides Hollow Nanoprisms via Self-Template Route as Electrode Material for Supercapacitors

Jihong Zhang, Ying Xu, Dongming Zeng*

College of Chemistry and Chemical Engineering, Central South University, Changsha, Hunan 410083, P. R. China.

*E-mail: dongmzeng@163.com

Received: 7 October 2018 / Accepted: 5 December 2018 / Published: 7 February 2019

Transition metal sulfides have got more concerns in the field of new energy devices. However, their practical application is vastly limited due to the high cost. In this report, we develop a simple self-templating approach to synthesize novel hollow CuCo_2S_4 nanoprism as a redox-type electrode. Owing to the hollow characteristic, the CuCo_2S_4 electrode offers a high specific capacity of 560 F g^{-1} at 1 A g^{-1} and displays 53.5% retention from 1 to 10 A g^{-1} in 3 M KOH aqueous electrolyte. This result provides a new route to prepare the other metal electrode materials for supercapacitors

Keywords: Hollow; Nanoprism ; CuCo_2S_4 ; Supercapacitor

1. INTRODUCTION

Supercapacitors have been highly considered as a promising application in energy conversion devices based on ultrahigh power density and long cycling life[1, 2]. Lately, because of the high electrochemical activity and lower electronegativity than the transition metal oxides, many efforts have been investigated on designing ternary transition metal chalcogenides [3-5]. Such as NiCo_2S_4 [6, 7], ZnCo_2S_4 [8-10], MnCo_2S_4 [11, 12] have been successfully synthesized and exhibited good electrochemical performances. However, the low content in the earth crust and high cost of metal elements (such as Mn, Zn, Ni, and Fe) limit their large-scale applications [13-16]. Therefore, it is urgent to seek eco-friendly and less expensive metal elements to prepare the sustainable electrode materials. Copper has been considered as fascinating candidates instead of precious metal element, due to its abundant natural resources, excellent chemical stability, and environmentally friendly capability[17, 18].

Nevertheless, there are little articles discussing for the preparation of copper cobalt sulfides for energy storage devices.

In recent advances, hollow nanostructured materials have been gained high attention due to the typical properties promoting the electrons between electrode and electrolyte moving quickly [19, 20]. However, the removal of templates is imperative to the template-assisted synthetic strategies, which result in the damage of the hollow structures[18]. Therefore, it is of importance to synthesize the hierarchical ternary metal sulfides with hollow feature through a simple method.

Inspired by the above discussions, we prepared the newfangled hollow CuCo_2S_4 nanoprism with a simple self-templating approach. A following anion-exchange process is implemented for the formation of the hollow structure. The electrochemical performance of the hierarchical CuCo_2S_4 nanoprism was studied. In particular, the as-obtained hollow prisms exhibited a high specific capacitance and outstanding cycling property. The result suggests that the hierarchical CuCo_2S_4 nanoprism materials hold great promising application for the supercapacitors.

2. EXPERIMENTAL

2.1. Preparation of hollow CuCo_2S_4 nanoprism

Briefly, cobalt (II) acetate monohydrate (170 mg), cobalt (II) acetate tetrahydrate (430 mg) and Polyvinylpyrrolidone (1500 mg, $M_w \approx 58000$) were dissolved in 100 mL ethanol solvent under magnetic stirrer for 1 h. Then, the mixture was refluxed for 8 h at 85 ° C. The precipitates were washed with absolute ethanol, and dried to produce Cu-Co precursors.

The obtained Cu-Co precursors (80 mg) were dispersed into 40 mL ethanol under ultrasonication for 10 min. Then 1.6 mmol thioacetamide (TAA) were added into the foregoing mixture with continued stirring for 30 min. The suspension was transferred into a 100 mL autoclave and heated hydrothermally at 120 °C for 6 h. The final product was collected by centrifugation with DI water several times. Finally, the as-obtained material was dried at 60 °C for 12 h. For comparisons, the nanostructures of CoS_2 have been synthesized using a similar method with the preparation of CuCo_2S_4 without the addition of copper salt.

2.2. Material Characterizations

The morphologies and internal structure of the materials were examined by a field-emission scanning electron-microscope (SEM, Nova Nano SEM 230) and transmission electron microscopy (TEM, FEI Titan G2 60-300). The crystallographic data of the products were confirmed with powder X-ray diffraction (XRD, Rint-2000) with Cu $K\alpha$ radiation ($\lambda = 1.5418 \text{ \AA}$). The valence states of elements were analyzed by X-ray photoelectron spectroscopy (XPS, ESCALAB 250Xi).

2.3. Electrochemical measurements

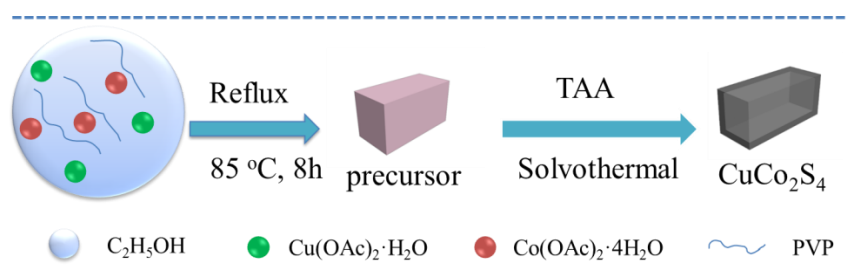
The working electrode was assembled with the CuCo_2S_4 material, acetylene black and PTEF in a weight ratio of 8:1:1. The black mixture was pressed onto nickel foam with mass loading of about 2 mg cm^{-2} . The specific capacitances were calculated from the galvanostatic charge-discharge (GCD) profile using the below formula

$$C = \frac{I \times \Delta t}{m \times \Delta V}$$

Where, C is specific capacitance ($\text{F} \cdot \text{g}^{-1}$), I is the discharge current (A), Δt is the discharge time (s), ΔV is the potential window (V), and m is the mass of the electrode materials (g).

3 . RESULTS AND DISCUSSION

The preparation of CuCo_2S_4 is schematically presented in scheme 1. The highly uniform copper-cobalt acetate hydroxide nanoprism as the precursors was obtained with a modified precipitation method using polyvinylpyrrolidone (PVP) as structural assistant agent. The Cu-Co precursor with solid structure chemically transformed into hierarchical CuCo_2S_4 nanoprisms with well-defined hollow interior through an anion-exchange treatment using Cu-Co precursors as a template and thioacetamide (TAA) as the sulfur sources.



Scheme 1. Schematic diagram of the synthesis process of CuCo_2S_4 .

The surface morphologies of the as-prepared Cu-Co precursor were captured by scanning electron microscopy (SEM). As depicted in Fig. 1(a, b), the SEM image of Cu-Co precursor particles display uniform tetragonal nanoprism with a glossy outside appearance. In addition, each tetragonal nanoprism are about $2\sim 3 \mu\text{m}$ in length and $0.5 \mu\text{m}$ in width. Figure 1c and d present the SEM image of CuCo_2S_4 sample. It is found that the surfaces of CuCo_2S_4 material are comparatively rough and composed by densely and numerous nano-grain. Particularly, Fig. 1c clearly clarifies the presence of several broken nanoprisms of CuCo_2S_4 that composed of the hollow interior structures. The micromorphologies of the tetragonal nanoprism of CuCo_2S_4 were also investigated with the transmission electron microscopy (TEM). As can be seen on Fig. 1 e and f, the internal configuration of CuCo_2S_4 is highly hollow, made up of plentiful polycrystalline particles, which agrees well with the results of SEM.

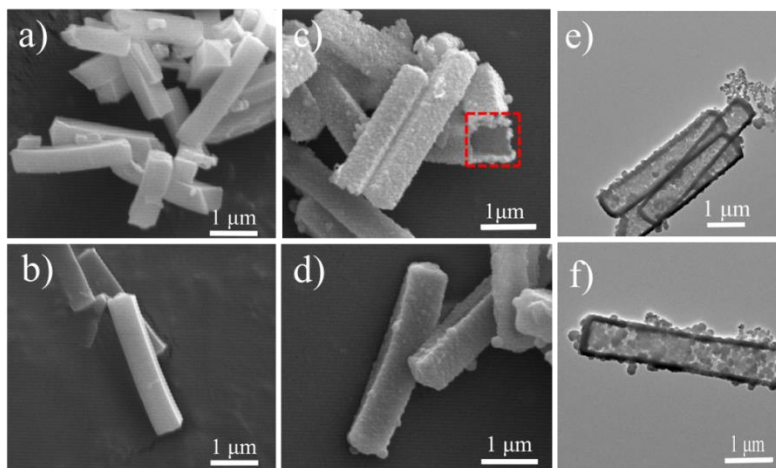


Figure 1. SEM images of: (a, b) the prisms Cu-Co precursors, (c, d) CuCo_2S_4 nanoprisms. TEM images: (e, f) the hierarchical CuCo_2S_4 nanoprisms.

For comparison, cobalt sulfides are prepared by similar routes as mentioned for CuCo_2S_4 , where no Cu salt was added. The SEM and TEM images of the resultant CoS_2 were observed in Fig. 2. The as-prepared cobalt acetate hydroxide precursor has a smooth surface with similar prism-like nanostructures (Fig. 2a). After sulfurizing hydrothermally, the nanoprism morphology of the precursors were mostly retained, and the surface of CoS_2 samples become relatively rough as well as CuCo_2S_4 electrode (Fig. 2b). As shown in Fig. 2c and d, the shadow in the center of CoS_2 clearly demonstrates the hollow feature.

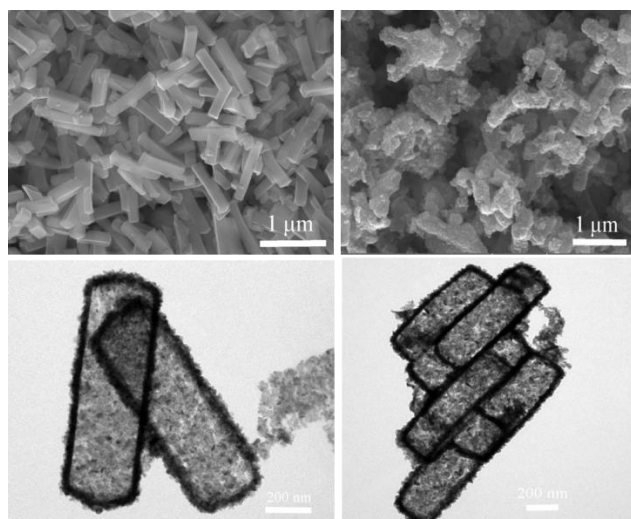


Figure 2. (a,b) Typical SEM of Co precursors and CoS_2 , respectively (c,d) TEM images of the CoS_2

The crystal structures of CuCo_2S_4 and CoS_2 are corroborated *via* XRD analysis (Fig. 3a). The diffraction peaks observed at 16.1° , 26.6° , 31.3° , 38.0° , 47.0° , 49.9° and 54.8° are corresponding to the (111), (022), (113), (004), (224), (115), and (044) crystal planes of CuCo_2S_4 (JCPDS card no. 42-1450), respectively. It is apparent that all diffraction peaks of the samples were identified and confirms the formation of single-phase CuCo_2S_4 . No peaks of the possible impurity were detected, reveals that the

high purity and well crystallinity of the as-obtained hollow CuCo_2S_4 structures. The diffraction peaks of CoS_2 are also consistent with the standard card of CoS_2 phase (JCPDS card no.75-0605).

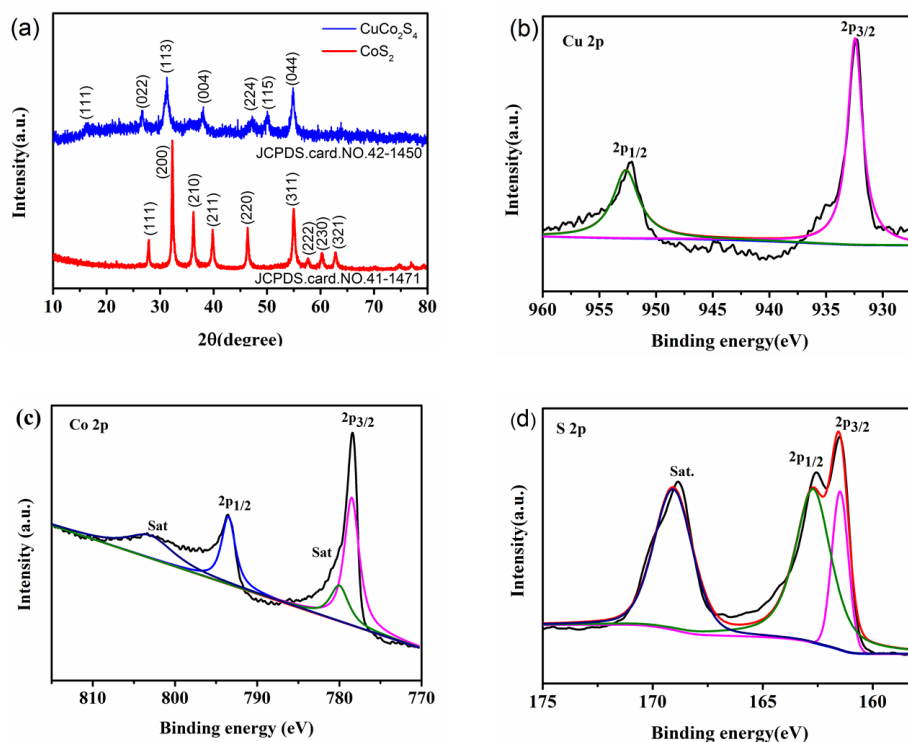


Figure 3. (a) XRD patterns of CuCo_2S_4 and CoS_2 samples, (b-d) XPS spectra of Cu 2p, Co 2p and S 2p, respectively.

To further analyze the surface valence of the hollow CuCo_2S_4 , X-ray photoelectron spectroscopy (XPS) measurement was also conducted (Fig. 3). The spectrum of Cu 2p is depicted in Fig. 3b, the two peaks observed at the binding energies of 952.2 and 932.3 eV ($\Delta E = 19.9$ eV), fitted with Cu 2p_{1/2} and Cu 2p_{3/2}, implying that the existence of Cu^{2+} specie [21]. The high-resolution Co 2p spectrum in Fig. 1c reveals that the energy bands at 781.1 and 796.3 eV belong to the Co 2p_{3/2} and Co 2p_{1/2}, respectively. The energy bands difference value of two main peaks is over 15 eV, demonstrates that the presence of both Co^{3+} and Co^{2+} species [22]. The two peaks of S 2p spectrum in Fig. 3d at 161.5 eV and 162.6 eV were indexed to S 2p_{3/2} and S 2p_{1/2}, respectively [23]. According to the above XPS analysis, the as-synthesized CuCo_2S_4 hollow nanoprism contains, Cu^{2+} , Co^{2+} , Co^{3+} and S^{2-} , which is supported with the previously reported work [24].

3.2. Study of electrochemical performance for CuCo_2S_4 electrodes

The electrochemical behavior of the hierarchical CuCo_2S_4 hollow architectures have been investigated in aqueous 3M KOH electrolyte as working electrode for supercapacitor. For comparison, the electrochemical properties of CoS_2 were also studied. Fig. 6a presents the CV curves of as-synthesized CuCo_2S_4 nanoprisms at different scan rates. The strong redox peaks different from ideal rectangular shapes reveal pseudocapacitive characteristics of the electrode materials rather than double-

layer characteristics. The possible electrochemical mechanisms of CuCo_2S_4 could be expressed by the following equations[25]:



Moreover, the shapes of CV curves have no obvious change with the scan rate increasing. Further, it manifests the enhanced rate capability and fast electron transport of the electrode materials. But the peaks position have the progressive shift, which are caused by the presence of diffusion-controlled reactions in CuCo_2S_4 [26]. Therefore, CuCo_2S_4 could be considered as the pseudocapacitive materials. Surprisingly, the including area of CV curve (Fig. 6c) for the CuCo_2S_4 is obviously the largest at a scan rate of 50 mV s^{-1} compared with CoS_2 , indicating that CuCo_2S_4 with the hierarchical structure possesses the higher specific capacitance and electrochemical reaction activity, which may ascribe to the high electrical conductivity and more new active sites created by copper introducing into CoS_2 .

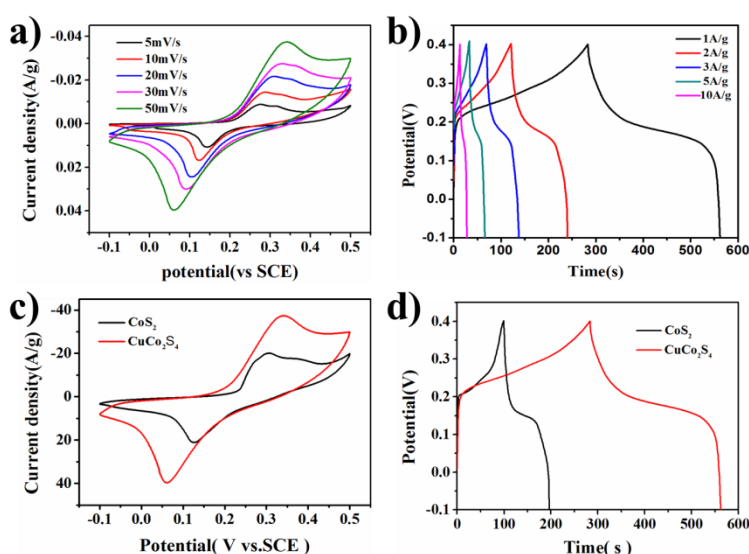


Figure 6. (a) CV curves of CuCo_2S_4 under various scanning rates, (b) charging-discharging curves of CuCo_2S_4 at various current densities. The electrochemical tests of CuCo_2S_4 and CoS_2 (c) CV curves at a scan rate of 50 mV s^{-1} (d) charging-discharging curves under a current density of 1 A g^{-1} ;

The GCD test was carried out to further verify the electrochemical behavior of CuCo_2S_4 . Fig. 6b exhibited the discharge profile of the obtained CuCo_2S_4 at diverse current rates. The distinct voltage plateau of CuCo_2S_4 electrodes reveals the dominant pseudocapacitive behavior, consisting with the above-mentioned conclusion from the CV curves [27, 28]. The symmetric shapes of GCD curves demonstrates the highly reversible redox reactions of the CuCo_2S_4 electrode[29]. Particularly, the longest discharge time of CuCo_2S_4 prisms compared with CoS_2 means that the capacity of CuCo_2S_4 hollow structures are larger in Fig. 6d. The reason for the as-obtained CuCo_2S_4 hollow prisms possessing the large electrochemical capacitance and excellent rate capability might own to the better conductivity, and more active sites that allow more efficient electron transfer for electrochemical reactions. As shown in

Table 1, CuCo_2S_4 electrode presents the better capacitive performance than other reported metal sulfides[30-34], which confirms the hollow nano-prism CuCo_2S_4 has the excellent application value.

Table 1. Comparison of the other metal sulfides material

Electrode materials	Morphologies	Current density (A/g)	Capacitance (F/g)	Ref.
CuCo_2S_4	hollow nano-prism	1	560	This work
Co9S8 on graphene paper	nanotube	1	536	[30]
copper-cobalt carbonate hydroxide	microsphere	1	397.3	[31]
CoS/CNT	nanoparticles	1	300	[32]
$\text{Cu}_2\text{S}/\text{RGO}$	nanoparticle	1	208	[33]
CuS	microsphere	2	204	[34]

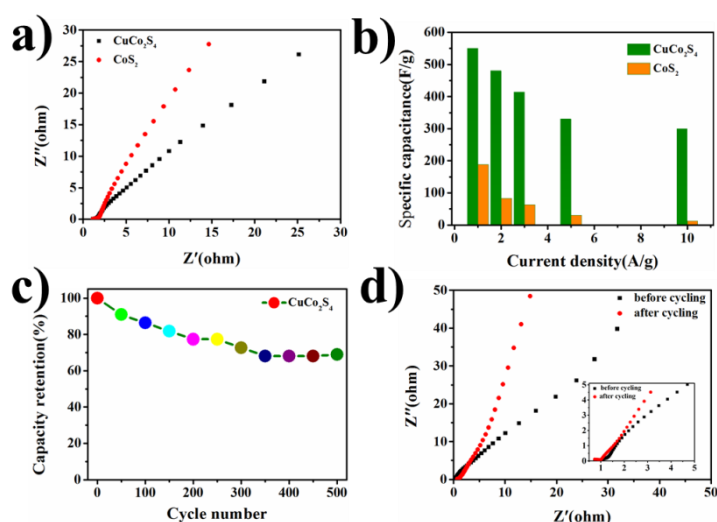


Figure 7. (a) Nyquist plots of CuCo_2S_4 and CoS_2 (b) Specific capacitance with various current density; (c) cycling performance of CuCo_2S_4 at 2.0 A g^{-1} (d) Nyquist plots of CuCo_2S_4 after cycling

For further clarify the conductivity and ions diffusion of the electrode materials, the electrochemical impedance spectroscopy (EIS) fitting was also utilized in the frequency range from 100 kHz to 0.01 Hz. As presented in Fig. 7a, it can be found that the Nyquist plots of CuCo_2S_4 performs the smallest slope compared to CoS_2 , implying the lowest internal resistance and much faster electron transfer[35]. These findings are indicative of excellent capacitive behavior and conductivity.

According to charge-discharge curves, the capacitances at different current densities are calculated in Fig. 7b. As expected, it can be found that CuCo_2S_4 hollow prisms retain about 53.5% original capacitance with the current density ranging from 1 to 10 A g^{-1} . On the contrast, the CoS_2 merely maintains 30.0% of the original value. The excellent retention rate of CuCo_2S_4 can be attributed to the high electrical conductivity, creating more active sites for CuCo_2S_4 nano-prism.

The cycling stability fitting is a crucial parameter in practical applications. Figure 7c. reveals the high and stable cycling performance of CuCo₂S₄ electrodes in 2 A g⁻¹, after 500 cycles completed, inheriting the 69% initial specific capacitances. These results may be in virtue of the hollow architecture of CuCo₂S₄, providing high active sites for electron transfer[36]. After cyclic measurements terminated, the EIS curve of CuCo₂S₄ electrode is carried out. As Figure 7d showed, the resistance of electrode rises. The reason is that hollow structure collapses after multiple charge and discharge.

4. CONCLUSIONS

In summary, this work prepared the novel hierarchical CuCo₂S₄ electrode materials with an efficient conversion method. The hollow CuCo₂S₄ nanoprisms were synthesized via a mild ion exchange process. Compared with CoS₂ nanoprism, the CuCo₂S₄ hollow nanoprisms exhibit the impressive specific capacitance (560 F g⁻¹ at 1 A g⁻¹) and stable cycling performance (69% retention after 500 cycles), resulting of the hollow CuCo₂S₄ structures further enhancing the conductivity, and also providing electroactive sites. Hence, these consequences clearly demonstrate that exploration of the hollow CuCo₂S₄ nanoprisms has significant novelty for supercapacitor.

ACKNOWLEDGMENTS

This work was funded by the National Natural Science Foundation of China (No. 21101172), and the Central South University Postdoctoral International Exchange Program.

References

1. S. Zheng, X. Li, B. Yan, Q. Hu, Y. Xu, X. Xiao, H. Xue, H. Pang, *Adv. Energy Mater.*, 7 (2017) 1602733.
2. J. Wang, J. Yang, T. Huang, W. Yin, *RSC Adv.*, 6 (2016) 103923.
3. X.Y. Yu, X.W. David Lou, *Adv. Energy Mater.*, 8 (2018) 1701592.
4. A. Namdarian, A.G. Tabrizi, A. Maseleno, A. Mohammadi, S.E. Moosavifard, *Int. J. Hydrogen Energy*, (2018).
5. A. Mohammadi, N. Arsalani, A.G. Tabrizi, S.E. Moosavifard, Z. Naqshbandi, L.S. Ghadimi, *Chem. Eng. J.*, 334 (2018) 66.
6. Y. Luan, H. Zhang, F. Yang, J. Yan, K. Zhu, K. Ye, G. Wang, K. Cheng, D. Cao, *Appl. Surf. Sci.*, 447 (2018) 165.
7. C. Xia, H.N. Alshareef, *Chem. Mater.*, 27 (2015) 4661.
8. P. Zhang, B.Y. Guan, L. Yu, X.W.D. Lou, *Angew. Chem. Int. Ed.*, 56 (2017) 7141.
9. C. Li, J. Balamurugan, N.H. Kim, J.H. Lee, *Adv. Energy Mater.*, 8 (2018) 1702014.
10. J. Li, B. Liu, M. Li, Q. Zhou, Q. Chen, C. Guo, L. Zhang, *Eur. J. Inorg. Chem.*, 2018 (2018) 3036.
11. A.M. Elshahawy, X. Li, H. Zhang, Y. Hu, K.H. Ho, C. Guan, J. Wang, *J. Mater. Chem. A*, 5 (2017) 7494.
12. H. Jia, Y. Song, J. Wu, W. Fu, J. Zhao, X. Liu, *Mater. Lett.*, 233 (2018) 55.
13. A.T. Aqueel Ahmed, B. Hou, H.S. Chavan, Y. Jo, S. Cho, J. Kim, S.M. Pawar, S. Cha, A.I. Inamdar, H. Kim, H. Im, *Small*, 14 (2018) e1800742.
14. H. Gao, Y. Li, H. Zhao, J. Xiang, Y. Cao, *Electrochim. Acta*, 262 (2018) 241.

15. Y. Wang, H. Li, Y. Zhang, Y. Peng, P. Zhang, J. Zhao, *Nano Res.*, 11 (2017) 831.
16. W. Xu, J. Lu, W. Huo, J. Li, X. Wang, C. Zhang, X. Gu, C. Hu, *Nanoscale*, 10 (2018) 14304.
17. M.D. Regulacio, Y. Wang, Z.W. Seh, M.-Y. Han, *ACS Appl. Nano Mater.*, 1 (2018) 3042.
18. Y. Zhu, X. Ji, H. Chen, L. Xi, W. Gong, Y. Liu, *RSC Adv.*, 6 (2016) 84236.
19. L. Yu, H. Hu, H.B. Wu, X.W. Lou, *Adv. Mater.*, 29 (2017).
20. X.-Y. Yu, L. Yu, X.W.D. Lou, *Adv. Energy Mater.*, 6 (2016) 1501333.
21. R. Jin, X. Liu, L. Yang, G. Li, S. Gao, *Electrochim. Acta*, 259 (2018) 841.
22. G. Cheng, T. Kou, J. Zhang, C. Si, H. Gao, Z. Zhang, *Nano Energy*, 38 (2017) 155.
23. S.G. Mohamed, I. Hussain, J.J. Shim, *Nanoscale*, 10 (2018) 6620.
24. R. Jin, Y. Cui, S. Gao, S. Zhang, L. Yang, G. Li, *Electrochim. Acta*, 273 (2018) 43.
25. H. You, L. Zhang, Y. Jiang, T. Shao, M. Li, J. Gong, *J. Mater. Chem. A*, 6 (2018) 5265.
26. J. Lin, H. Jia, H. Liang, S. Chen, Y. Cai, J. Qi, C. Qu, J. Cao, W. Fei, J. Feng, *Chem. Eng. J.*, 336 (2018) 562.
27. S.E. Moosavifard, S. Fani, M. Rahmanian, *Chem Commun (Camb)*, 52 (2016) 4517.
28. Y. Zhu, X. Chen, W. Zhou, K. Xiang, W. Hu, H. Chen, *Electrochim. Acta*, 249 (2017) 64.
29. C. Wang, K. Guo, W. He, X. Deng, P. Hou, F. Zhuge, X. Xu, T. Zhai, *Sci. Bull.*, 62 (2017) 1122.
30. D. Xiong, X. Li, Z. Bai, J. Li, Y. Han, D. Li, *Chemistry*, 24 (2018) 2339.
31. S.H. Guo, P.W. Yuan, J. Wang, W.Q. Chen, K.Y. Ma, F. Liu, J.P. Cheng, *J. Electroanal. Chem.*, 807 (2017).
32. C.V.V. Muralee Gopi, S. Ravi, S.S. Rao, A. Eswar Reddy, H.J. Kim, *Sci. Rep.*, 7 (2017) 46519.
33. Z.J. Li, B.C. Yang, X.W. Lv, Y.C. Li, L. Wang, *Appl. Surf. Sci.*, 370 (2016) 508.
34. J. Zhang, H. Feng, J. Yang, Q. Qin, H. Fan, C. Wei, W. Zheng, *ACS Appl. Mater. Interfaces*, 7 (2015) 21735.
35. J. Shen, J. Tang, P. Dong, Z. Zhang, J. Ji, R. Baines, M. Ye, *RSC Adv.*, 6 (2016) 13456.
36. M.-L. Li, K. Xiao, H. Su, N. Li, Y.-P. Cai, Z.-Q. Liu, *ChemElectroChem*, 5 (2018) 2496.